Available online at www.sciencedirect.com
ScienceDirect
Trans. Nonferrous Met. Soc. China 22(2012) 2027−2031
Transactions of Nonferrous Metals Society of China
www.tnmsc.cn

Hot pressing densification of WC−Mo_xC binderless carbide

ZHANG Li[1], CHEN Shu[2], SHAN Cheng[1], HUANG Fang-jie[1], CHENG Xin[1], MA Yun[1]

1. State Key Laboratory of Powder Metallurgy, Central South University, Changsha 410083, China;
2. Changsha Mining and Metallurgy Research Institute Co., Ltd., Changsha 410012, China

Received 24 August 2011; accepted 15 December 2011

Abstract: WC−6Mo_xC−0.47Cr_3C_2−0.28VC binderless carbide was prepared by hot pressing (1700 °C, 20 MPa). The sample was observed and analyzed by scanning electron microscopy, energy dispersive X–ray spectroscopy and X–ray diffraction. The results show that during the hot pressing process, W atoms dissolve substantially into the Mo_xC crystal lattices; whilst, the reverse dissolution of Mo atoms into the WC crystal lattices takes place. Consequently, the main phase and binder phase structure are formed. The phase compositions of the main phase and binder phase are a WC-based solid solution containing Mo and a Mo_2C-based solid solution containing W, respectively. The isotropic dissolution and precipitation of W and Mo atoms do not result in substantial carbide coarsening. The mechanism for the densification was discussed.

Key words: binderless carbide; hot pressing; diffusion behavior; densification; grain growth; WC−Mo_xC

1 Introduction

Due to the unique combination of strength, toughness and hardness, cemented carbides are universally applied to cutting, mining and forming tools, as well as to high-performance wear resistant parts. In general, cemented carbides consist of a hard phase (primarily WC) and a binder phase (ferrous metal). These binder phases, however, are inferior to the carbide phases in hardness. Particularly, the corrosion and oxidation of cemented carbides start in the binder phase first. Binderless carbides have been developed as a complement to the conventional cemented carbides for use in corrosive environments where the metal binder degrades. Binderless carbides can be divided into two groups. The one consists of pure carbide, e.g., WC [1], TiC [2], TaC [3] and NbC [4]; the other consists of WC phase and a mixed transition metal carbide/carbonitride binder phase, e.g., WC−TiC [5], WC−TiC−TaC [6], WC−VC [7], WC−(Ti, W)(C, N) [8] and WC−Mo_2C [6,9]. Among the binderless carbides, WC−Mo_xC binderless carbides have good combination property and higher performance-price ratio [6,10]. The researches available on the WC−Mo_xC binderless carbides were mainly focused on their properties. Evidently, the investigation of the hot pressing densification and the related grain growth behavior of WC−Mo_xC binderless carbides can provide an insight into the optimization of the preparation technique and the understanding of their property characteristics. Moreover, it can also provide an insight into the fundamental aspects of the densification mechanism of solid phase sintering and the grain growth mechanism of cemented carbides.

2 Experimental

Ultrafine tungsten carbide powder pre-doped with 0.5%Cr_3C_2−0.3%VC (in mass fraction) and fine molybdenum carbide (Mo_xC) powder were used as the raw materials. Molybdenum carbide was pretreated for 36 h by ball milling in hexane to obtain a particle size that matches the one of tungsten carbide powder. Table 1 summarizes the characteristics of the powders used in this study.

Powders corresponding to the composition of WC−6%Mo_xC−0.47%Cr_3C_2 −0.28%VC (in mass fraction)

Foundation item: Project (51074189) supported by the National Natural Science Foundation of China; Project (20100162110001) supported by Research Fund for the Doctoral Program of Higher Education of China; Project (2011BAE09B02) supported by the National Key Technology R & D Program of China

Corresponding author: ZHANG Li; Tel: +86-731-88876424; E–mail: zhangli@csu.edu.cn

DOI: 10.1016/S1003-6326(11)61424-6

Table 1 Characteristics of raw materials

Powder	S_{BET}/ ($m^2 \cdot g^{-1}$)	d_{BET}/ μm	FSSS/ μm	Total carbon/%	Free carbon /%	Phase composition
Doped WC	3.00	0.127	–	6.15	0.07	100%WC
Mo_xC	–	–	1.92	6.02	0.17	97.7%Mo_2C+ 2.3%MoC

S_{BET}: BET specific surface area; d_{BET}: calculated BET grain size; FSSS: Fischer sub-sieve size; phase composition was determined by XRD.

and paraffin wax-based macromolecule compounds were wet milled in a multicomponent ball-milling organic medium for 72 h in a conventional ball mill. The mass ratio of milling media (cemented carbide balls) to charge was 4:1. Hot pressing of the sample at the temperature of 1700 °C and a pressure of 20 MPa for 60 min was carried out in a high-multi 10000 vacuum hot pressing equipment. The final sizes of the hot-pressed sample were 37.4 mm in diameter and 15 mm in height. For the observation and analysis, a cubic sample with dimensions of 10 mm×10 mm×10 mm was cut out with a diamond saw from the hot-pressed sample. The relative density and Vickers hardness HV_{10} of the sample are 98% and 24157 MPa, respectively.

The phase identification was conducted on a Rigaku Dmax/2550 X–ray diffractometer. A MDI Jade 6.0 analysis software developed by Materials Data Inc. was used to analyze the X–ray diffraction patter. The microstructure was observed and analyzed on a JEOL JSM–6490 LV scanning electron microscope (SEM) and the attached EDAX Genesis XM4 Neptune energy dispersive X–ray spectroscope (EDS). The observation and analysis were carried out directly on the polished surface.

3 Results and discussion

3.1 Microstructure analysis

Figure 1 shows the SEM images of WC−6%Mo_xC−0.47%Cr_3C_2−0.28%VC (WC−6Mo_xC−0.47Cr_3C_2−0.28VC) binderless carbide. It is known that the high sintering temperature does not result in remarkably anisotropic carbide coarsening. The average grain size of the binderless carbide is less than 0.8 μm. EDS analysis results of the micro zone 1 and the positions 2−5 of the cross center shown in Fig. 1(b) are given in Fig. 2. The micro-zone 1 and position 3 locate on the main phase in bright color. The positions 2, 4 and 5 locate on the binder phase in dark color. Both Mo and W are detected in all the cases shown in Fig. 2. Among them, much stronger strength of the diffraction peak of

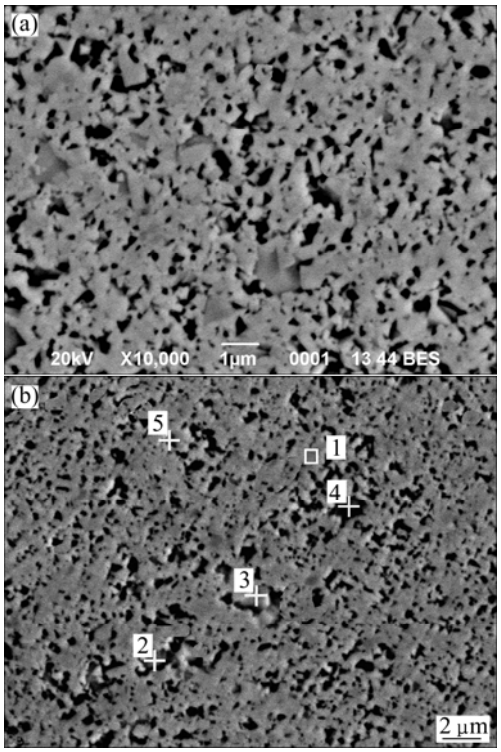

Fig. 1 SEM images of WC−6Mo_xC−0.47Cr_3C_2−0.28VC binderless carbide

Mo is detected in position 4. The EDS results show a mole ratio of W to Mo 1.16:1. Considering the fact that the distance from the center of the position 4 to the neighboring phase reaches about 1 μm, the effect of the neighboring phase on the EDS analysis result is relatively little, and thus the result must approach to its nominal composition. From the strength of the diffraction peak it is known that there are a small amount of Mo atoms in the main phase and a large amount of W atoms in the binder phase. The EDS analysis results show a great consistency with the established knowledge that the W atoms and Mo atoms are substitutable in the related carbide [6,9,11,12]. It can be deduced that the reverse dissolution of Mo atoms into the WC crystal lattices must facilitate the dissolution of W atoms into the crystal lattices of molybdenum carbide. Combining the EDS analysis results and the relative density as high as 98%, it can be deduced that the mechanism for the densification of WC−6Mo_xC−0.47Cr_3C_2−0.28VC through solid phase sintering is dominated by the bulk diffusion between W and Mo atoms in a nonequilibrium manner. Moreover, the high temperature (1700 °C) and high pressure (20 MPa) can induce a viscosity/plastic flow of the phases, which facilities the densification [13,14].

From the microstructure of WC−3.65TiC−2.45TaC−0.47Cr_3C_2−0.28VC binderless carbide prepared under the same technique conditions [15], it is known that part of the WC grains take the shape of platelet indicated by the

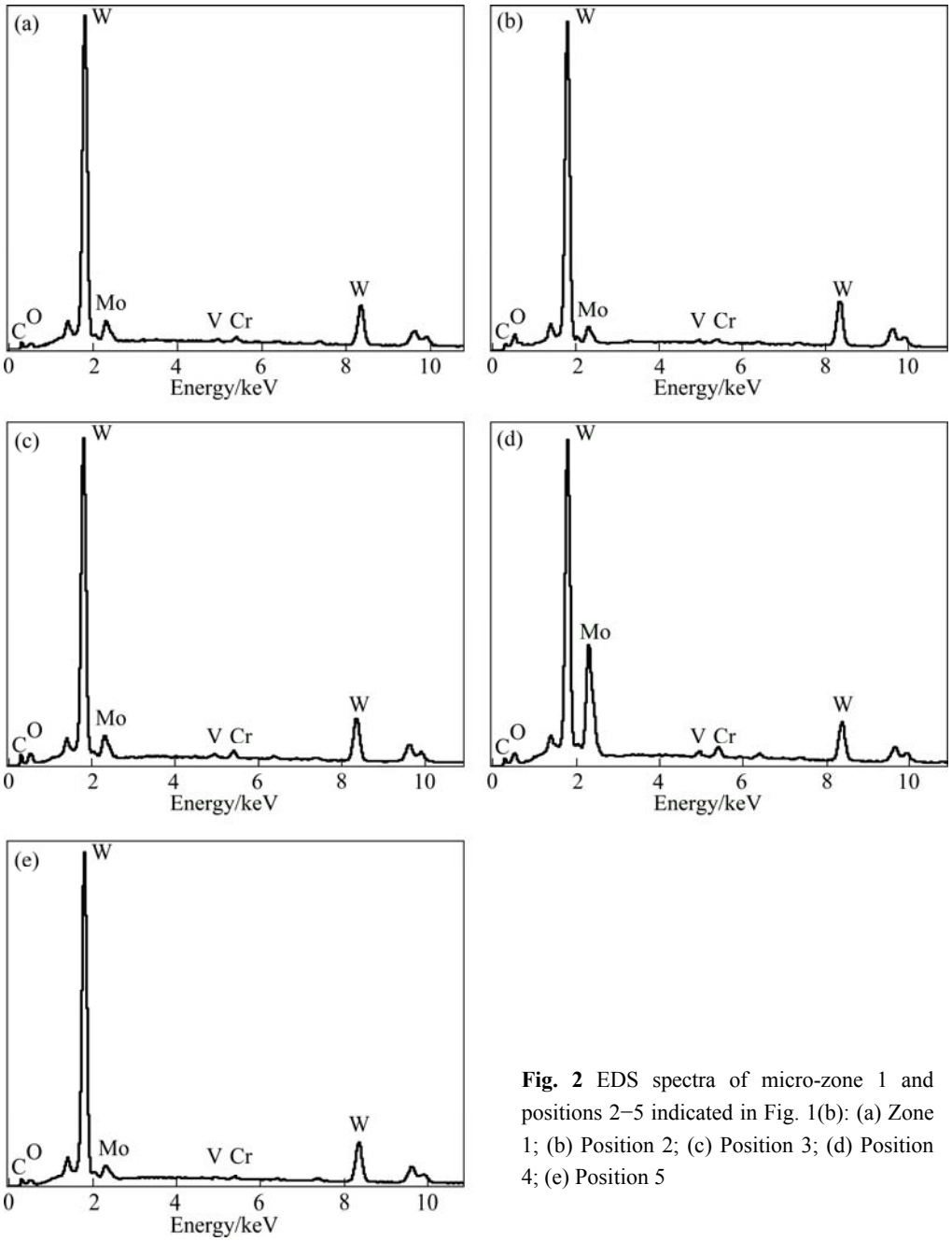

Fig. 2 EDS spectra of micro-zone 1 and positions 2−5 indicated in Fig. 1(b): (a) Zone 1; (b) Position 2; (c) Position 3; (d) Position 4; (e) Position 5

arrows shown in Fig. 3. The formation of platelet WC grains is considered to be the results of the anisotropic dissolution and precipitation of W atoms in the binder phase [16,17]. By comparing Fig. 1(a) and Fig. 3, substantial difference in the grain shape of the main phase can be identified. This fact suggests that the dissolution and precipitation of W and Mo atoms during the hot pressing process of WC−6Mo$_x$C−0.47Cr$_3$C$_2$−0.28VC tend to be isotropic. This isotropic dissolution and precipitation must be the reason behind the inhibition of the carbide coarsening.

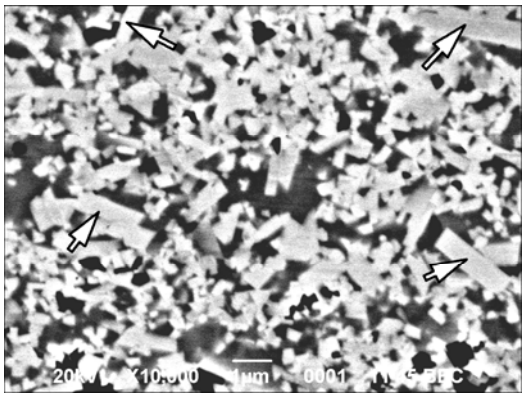

Fig. 3 SEM image of WC−3.65TiC−2.45TaC−0.47Cr$_3$C$_2$−0.28VC binderless carbide [15]

3.2 Phase composition analysis

The XRD patterns of WC−6Mo$_x$C−0.47Cr$_3$C$_2$−

0.28VC binderless carbide and the molybdenum carbide raw material are shown in Fig. 4. From the PDF cards in the XRD diffraction database attached to the MDI Jade 6.0 analysis software, it is known that for WC (PDF cards: 89—2727, 73—0471, 72—0097, 51—0939, 65—8828, 65—4539), MoC (PDF cards: 65—8765, 65—6664) and $WMoC_2$ (PDF cards: 65—8770), they share the same set of characteristic peaks. The same is true for Mo_2C (PDF cards: 71—0242, 77—0720, 65—8766, 72—1683, 89—2669, 79—0744, 89—3104) and W_2C (PDF cards: 20—1315, 35—0776, 65—3896, 89—2371, 79—0743). All the similar phases with overlapping diffraction peaks make the phase identification of $WC-6Mo_xC-0.47Cr_3C_2-0.28VC$ binderless carbide a little bit complicated. From the point of the nominal composition of the binderless carbide, the EDS analysis results of the main phase, as well as the strength characteristic of the corresponding diffraction peaks, it can be concluded that the main phase is a WC- based solid solution containing Mo. Although it was reported that W_2C phase can exist in binderless carbides [15,18,19], according to the XRD pattern of molybdenum carbide raw material, the EDS analysis results of the binder phase, as well as the strength characteristic of the corresponding diffraction peaks, it is known that the binder phase is a Mo_2C-based solid solution containing W. The XRD quantitative analysis result shows that the mass fractions of the main phase and the binder phase are 74.4% and 25.6%, respectively. Evidently, the high mass fraction of the binder phase is the result of the high solid solubility of W caused by the high sintering temperature and pressure. We have shown that $WC-6Mo_2C-0.47Cr_3C_2-0.28VC$ binderless carbide exhibits better corrosion resistance to H_2SO_4 solution (pH=1), Na_2SO_4 solution (pH=7) and NaOH solution (pH=13) than $WC-0.5Cr_3C_2-0.3VC$ binderless carbide prepared under the same condition [10]. From this investigation, it can be deduced that the improvement of the corrosion resistance must be strongly related with the formation of the solid solution of the main phase and the binder phase.

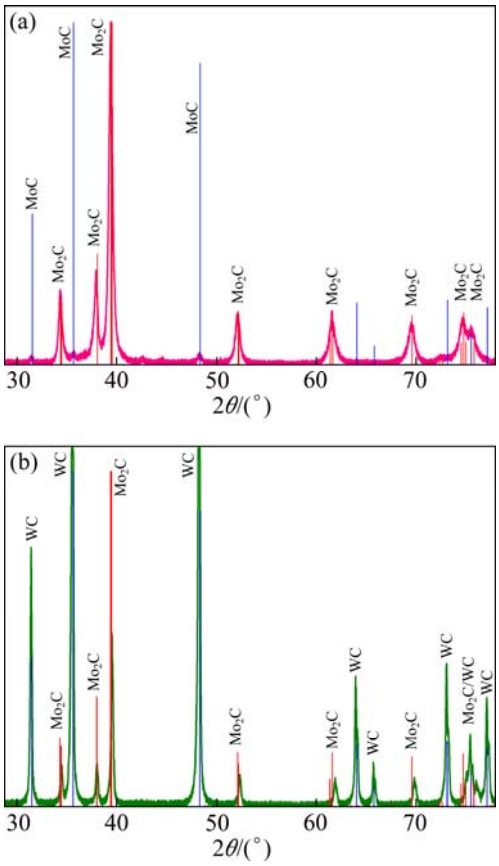

Fig. 4 XRD patterns of molybdenum carbide raw material (a) and $WC-6Mo_xC-0.47Cr_3C_2-0.28VC$ binderless carbide (b)

4 Conclusions

1) During the high temperature (1700 °C) and high pressure (20 MPa) solid phase sintering process of $WC-6Mo_xC-0.47Cr_3C_2-0.28VC$ binderless carbide, W atoms dissolve substantially into the crystal lattices of molybdenum carbide. Whilst, the reverse dissolution of Mo atoms into the WC crystal lattices takes place. Consequently, a structure with WC-based solid solution main phase containing Mo and Mo_2C-based solid solution binder phase containing W is formed, in which the mass fraction of the binder phase is as high as 25.6%.

2) The mechanism for the densification through solid phase sintering is dominated by the bulk diffusion between W and Mo atoms in a nonequilibrium manner and a viscosity/plastic flow of the phases caused by the high temperature and high pressure.

3) The isotropic dissolution and precipitation of W and Mo atoms at high temperature and high pressure condition do not result in substantial carbide coarsening.

References

[1] TSAI K M. The effect of consolidation parameters on the mechanical properties of binderless tungsten carbide [J]. International Journal of Refractory Metals and Hard Materials, 2011, 29(2): 188−201.

[2] SHON I J, KIM B R, DOH J M, YOON J K. Consolidation of binderless nanostructured titanium carbide by high-frequency induction heated sintering [J]. Ceramics International, 2010, 36(6): 1797−1803.

[3] KIM B R, WOO K D, DOH J M, YOON J K, SHON I J. Mechanical properties and rapid consolidation of binderless nanostructured tantalum carbide [J]. Ceramics International, 2009, 35(8): 3395−3400.

[4] KIM B Y, WOO K D, YOON J K, DOH J M, SHON I J. Mechanical properties and rapid consolidation of binderless niobium carbide [J]. Journal of Alloys and Compounds, 2009, 481(1−2): 573−576.

[5] KIM H C, KIM D K, WOO K D, KO I Y, SHON I J. Consolidation of binderless WC−TiC by high frequency induction heating sintering

[J]. International Journal of Refractory Metals and Hard Materials, 2008, 26(1): 48−54.

[6] ENGQVIST H, BOTTON G A, AXÉN N, HOGMARK S. Microstructure and abrasive wear of binderless carbides [J]. Journal of the American Ceramic Society, 2000, 83(10): 2491−2496.

[7] HUANG S G, VANMEENSEL K, van der BIEST O, VLEUGELS J. Binderless WC and WC−VC materials obtained by pulsed electric current sintering [J]. International Journal of Refractory Metals and Hard Materials, 2008, 26(1): 41−47.

[8] KANG Y J, KANG S H. WC-reinforced (Ti, W)(CN) [J]. Journal of the European Ceramic Society, 2010, 30 (3): 793−798.

[9] KIM H C, PARK H K, JEONG I K, KO I Y, SHON I J. Sintering of binderless WC−Mo_2C hard materials by rapid sintering process [J]. Ceramics International, 2008, 34, (6): 1419−1423.

[10] MA Yun, ZHANG Li, SHAN Cheng. Electrochemical corrosion behaviors of binderless carbides [J]. Materials Science and Engineering of Powder Metallurgy, 2011, 16(6): 820−826. (in Chinese)

[11] JOHANSSON S A E, WAHNSTRÖM G A. Computational study of thin cubic carbide films in WC/Co interfaces [J]. Acta Materialia, 2011, 59(1): 171−181.

[12] HUGOSSON H W, ENGQVIST H. The connection between the electronic structure and the properties of binderless tungsten carbides [J]. International Journal of Refractory Metals and Hard Materials, 2003, 21(1): 55−61.

[13] LIU Bin-bin, LU Yan-na, XIE Jian-xin. Fabrication of tungsten/copper functionally gradient materials with nearly full density by hot press [J]. The Chinese Journal of Nonferrous Metals, 2007, 17(9): 1410−416. (in Chinese)

[14] JEONG Y K, NIIHARA K. Microstructure and properties of alumina-silicon carbide nanocomposites fabricated by pressureless sintering and post hot-isostatic pressing [J]. Transactions of Nonferrous Metals Society of China, 2011, 21(S1): 1−6.

[15] ZHANG Li, SHAN Cheng, CHEN Shu, NAN Qing. Hot pressing densification and grain growth behavior of WC−TiC−TaC binderless carbide [J]. Materials Science and Engineering of Powder Metallurgy, 2011, 16(5): 781−786. (in Chinese)

[16] ZHANG Li, CHEN Shu, ZHANG Chuan-fu. Cemented carbide with WC platelet-enhanced bi-model structure [J]. Chinese Journal of Rare Metals, 2004, 28(6): 979−982. (in Chinese)

[17] ZHANG Li, CHEN Shu, WANG Yuan-jie. Tungsten carbide platelet-containing cemented carbide with yttrium containing dispersed phase [J]. Transactions of Nonferrous Metals Society of China, 2008, 18(1): 104−108.

[18] DEMIRSKYI D, RAGULYA A, AGRAWAL D. Initial stage sintering of binderless tungsten carbide powder under microwave radiation [J]. Ceramics International, 2011, 37(2): 505−512.

[19] GIRARDINI L, ZADRA M, CASARI F. SPS, binderless WC powders, and the problem of sub carbide [J]. Metal Powder Report, 2008, 63(4): 18−22.

WC−Mo_xC 无金属粘结相硬质合金的热压致密化

张 立[1]，陈 述[2]，单 成[1]，黄方杰[1]，程 鑫[1]，马 鋆[1]

1. 中南大学 粉末冶金国家重点实验室，长沙 410083；
2. 长沙矿冶研究院有限责任公司，长沙 410012

摘 要：采用 1700 °C、20 MPa 热压工艺，制备 WC−6Mo_xC−0.47Cr_3C_2−0.28VC 无金属粘结相硬质合金。采用 X 射线衍射技术分析合金的物相成分，采用扫描电镜与能谱仪对合金的微观组织结构特征进行分析。结果表明，在高温、高压固相烧结过程中，发生了 WC 中的 W 原子向 Mo_xC 中的大量固溶以及 Mo_xC 中的 Mo 原子向 WC 中的反向固溶，导致含 Mo 的 WC 基固溶体与含 W 的 Mo_2C 基固溶体的形成。W、Mo 原子之间的溶解－析出行为不存在明显的各向异性，没有导致合金晶粒的显著长大。并讨论了合金的固相烧结致密化机制。

关键词：无粘结相硬质合金；热压；扩散行为；致密化；晶粒生长；WC−Mo_xC

(Edited by LI Xiang-qun)